

TRANSITION, PRESSURE GRADIENT, SUCTION, SEPARATION
AND STABILITY THEORY

by

J.L. van Ingen

Paper nr 20 in AGARD CP-224
Copenhagen 1977

TRANSITION, PRESSURE GRADIENT, SUCTION, SEPARATION AND STABILITY THEORY.

J.L. van Ingen

Department of Aerospace Engineering, Delft University of Technology, Kluyverweg 1, Delft, The Netherlands.

SUMMARY.

A semi-empirical method is presented for the prediction of transition in two-dimensional incompressible flows with pressure gradient and suction. Included is the case of the laminar separation bubble, where transition is preceded by laminar separation.

The method employs linear stability theory to calculate the amplification factor σ for unstable disturbances in the laminar boundary layer. (σ is defined as the natural logarithm of the ratio between the amplitude of a disturbance at a given instant or position to the amplitude at neutral stability). It is found that at the experimentally determined transition position the calculated amplification factor for the critical disturbances attains nearly the same value (about 10) in many different cases for flows with low free stream turbulence levels. An attempt is made to include the effects of higher free stream turbulence levels by allowing the critical amplification factor to decrease with increasing free stream turbulence.

NOTATION.

The symbols used are the conventional ones for boundary layer and stability theory. To avoid confusion a few of them are mentioned specifically below.

c reference length

$$m = -\frac{\theta}{v} \frac{dU}{dx}$$

$$R_c = \frac{U_\infty c}{v}$$

$$R_\theta = \frac{U\theta}{v}$$

U velocity at edge of boundary layer

U_∞ reference velocity

$$\bar{U} = U/U_\infty$$

x or s distance along contour of body

x_c distance along chord

$$\bar{x} = \frac{x}{c}$$

$$\bar{s} = s/c$$

subscript sep refers to conditions at separation.

1. LINEAR STABILITY THEORY.

In linear stability theory a given two-dimensional laminar main flow is subjected to sinusoidal disturbances with a disturbance stream function:

$$\psi = \phi(y) e^{i(\alpha x - \omega t)} \quad (1)$$

For the spatial mode ω is real and α is complex $\alpha = \alpha_r + i \alpha_i$. This leads to a factor $e^{-\alpha_i x}$ in the disturbance amplitude and σ follows from:

$$\sigma = \int_{x_0}^x -\alpha_i dx = \frac{U_\infty c}{v} 10^{-6} \int_{\bar{x}_0}^{\bar{x}} T \bar{U} d\bar{x} \quad (2)$$

where x_0 is the streamwise position where the disturbance with frequency ω is neutrally stable. T is defined as:

$$T = \frac{-\alpha_i \theta}{R_\theta} 10^6 \quad (3)$$

In the temporal mode the same expression (2) for σ is found with a different definition for T. It is clear that σ is a function of x and ω for a given boundary layer; σ can be calculated as soon as stability diagrams are available for the velocity profiles for successive streamwise positions x . For a long time Pretsch' stability diagrams, for the temporal stability of the Hartree similar velocity profiles, have been the only source of detailed stability data for flows with non-zero pressure gradient [6]. Results for the spatial stability of the Hartree flows have been given by Wazzan, Okamura and Smith [7] and Kümmerer [8], stability diagrams for the reversed flow solutions of the Falkner-Skan equation have been obtained by Taghavi and Wazzan [11].

2. STABILITY AND TRANSITION OF THE FLAT PLATE BOUNDARY LAYER.

Fig. 1a shows σ for the flat plate according to Pretsch for different non-dimensional frequencies $\frac{\omega V}{U^2}$. The envelope of these curves gives the maximum value of σ for each streamwise position. In what follows we will in general mean this maximum value when we mention σ . The curve labelled 3 in fig. 1b is the envelope according to [7] and [8]; the curve labelled 2 will be discussed later. A well known result for the experimentally determined transition region is due to Schubauer and Skramstad [12]. They find for low free stream turbulence levels Reynolds numbers at beginning and end of transition equal to 2.8×10^6 and 3.9×10^6 respectively. To these Reynolds numbers correspond certain values σ_1 and σ_2 for σ which are indicated in table 1.

3. FIRST VERSION OF THE PREDICTION METHOD (1956).

The present author used Pretsch charts in [1] to calculate amplification factors for an airfoil section (EC 1440) at different values of angle of attack and Reynolds number.

It was shown that $\sigma_1=7.6$ and $\sigma_2=9.7$ gave a reasonably accurate prediction of the transition region. Smith and Gamberoni [3], defining a transition point rather than a transition region found that $\sigma=9$ would correlate different transition experiments reasonably well.

Although it is clear that a transition criterion should be based on the actual amplitude of the disturbance, rather than on an amplification ratio, the method has been used extensively. Its success may have been due to the fact that the initial disturbances - due to free stream turbulence for instance - have been about the same for the cases investigated.

Another way to explain the success of the method may be that σ is a suitable factor in which different factors, known to influence transition, may be correlated.

4. SECOND VERSION, ALSO APPLICABLE TO FLOWS WITH SUCTION (1965).

In 1965 the present author extended the method to the case of two-dimensional incompressible boundary layers with suction [2]. Since at that time the Pretsch charts were still the only source of detailed information on amplification rates, some drastic simplifying assumptions had to be made. First it was assumed that all possible stability diagrams, including those for suction boundary layers, formed a one-parameter family with the critical Reynolds number as parameter. Furthermore, it was assumed that the critical Reynolds number could be determined from an approximation formula due to Lin. The suction boundary layer was calculated using a two-parameter method of integral relations. This necessitated a new "calibration" of the transition prediction method against the flat plate without suction, leading to curve 2 in fig. 1b with $\sigma_1=9.2$ and $\sigma_2=11.2$.

To facilitate the amplification calculations using a computer Pretsch' charts have been brought in a tabular form. Fig. 2 shows an application to the EC 1440 airfoil; some results for an airfoil with suction through a porous surface are shown in figs. 3 and 4.

In view of the many simplifying assumptions which had to be made the correspondence between theory and experiment may be considered to be good.

Since 1965 this version of the method has been included in a computer program for the analysis and design of airfoil sections [13]. The streamwise position for the end of the transition region (determined by σ_2) has been used as the starting point for the turbulent boundary layer calculation.

It has been found that an improved transition prediction could be made by allowing the value for σ_2 to vary from 11.2 for favourable and zero pressure gradient to about 20 for boundary layers near separation. (In the last version σ_2 is again more nearly constant). In general the position of transition was predicted within a few percent of the chord. An example of application of this airfoil analysis program taken from [14] is shown in fig. 5. The airfoil investigated is that of the horizontal tailplane of the Italian sailplane M300 "Aliante". The airfoil was designed by cambering the NACA 63₃-018 section. The tailplane is produced through an extrusion process which caused appreciable surface waviness. An actual specimen of this tailplane was tested as a two-dimensional model in the low speed wind tunnel of the Department of Aerospace Engineering at Delft. It was found that the surface waves caused early transition in a certain angle of attack range; this could be remedied by smoothing the forward part of the surface. The calculation, starting from the airfoil coordinates for both conditions, predicted this change quite well.

It should be stressed again that the present method may be considered as a method to correlate different transition experiments. The calculated amplification factors need not have a precise physical meaning. It is however a definite advantage of the method that linear stability theory is used which has proved to be a valuable tool to describe the early phases of the transition process. It should also be observed that inaccuracies in one of the elements of the method (viz. boundary layer calculation; calculation of the critical Reynolds number using Lin's formula; the stability diagrams used) may have been neutralized by inaccuracies in another element. Hence if any element is changed, a new calibration is necessary. An important imperfection in the second version of the method was that the stability characteristics in laminar separation bubbles were obtained by extrapolation from the attached flow. This may have been the cause of the high values of σ_2 required to predict accurately the end of the transition region in boundary layers near to or after separation.

5. A SHORT CUT METHOD TO PREDICT TRANSITION IN SEPARATION BUBBLES.

In [5] the present author published a short-cut method to predict transition in separated flow. The method is based on the stability diagrams for reversed flows due to Taghavi and Wazzan [11] and some additional calculations by the present author for the limiting stability characteristics when $R_\theta \rightarrow \infty$, using the inviscid stability equation (Rayleigh equation). The following assumptions are made:

- 1) U , θ and R_θ in the separation bubble are independent of x and equal to their values at separation. Then a constant value of ω also means a constant value of $\frac{\omega\theta}{U}$.
- 2) The separation streamline is straight, and leaves the wall at an angle γ determined by:

$$\text{tg}(\gamma) = \frac{B}{\left(\frac{U\theta}{v}\right)_{\text{sep}}} \quad (4)$$

where B is a constant equal to 17.5.

- 3) The Reynolds number is so high with respect to the (very low) critical Reynolds number that the stability characteristics are given with sufficient accuracy by the limiting values determined from the inviscid stability equation.

Then $-\alpha_1\theta$ only depends on the value of $\frac{\omega\theta}{U}$ and the velocity profile shape parameter.

Finally we introduce the shape parameter $z = g \times m_{\text{sep}}$, where g is the height of the separation streamline above the wall divided by θ and $m_{\text{sep}} = -\frac{\theta^2}{v} \frac{dU}{dx}$ at separation. Then the integration w.r.t. x in (2) can be replaced by an integration w.r.t. to z leading to:

$$\sigma = \frac{(R_\theta)_{\text{sep}}}{B \cdot m_{\text{sep}}} \int (-\alpha_1\theta) dz \quad (5)$$

(a similar result may be obtained for a small region upstream of separation when integration w.r.t.

$\lambda = \frac{\tau_o\theta}{\mu U}$ is used).

The inviscid instability for different values of the Hartree parameter β is shown in figs 6 and 7. Values of $10^4 \int (-\alpha_1\theta) dz$ are shown in fig. 8 for different values of $\frac{\omega\theta}{U}$ together with the envelope giving the

maximum value I of the integral as a function of z . (See also table 2). Hence in the separation bubble we have:

$$\sigma = \frac{10^{-4} (R_{\theta})_{\text{sep}} I}{B.m_{\text{sep}}} \quad (6)$$

Using this short-cut method it was found in [5] that σ_2 for separation bubbles on an airfoil in a small "noisy" tunnel was about 12.5 (fig. 9). For separation bubbles on a circular cylinder with a tapered tail in the large low turbulence wind tunnel, values of σ_2 between 13.2 and 15.7 were found, depending on the wind speed. Using the same short-cut method Van der Meulen [15] obtained $\sigma_2=7$ for a body of revolution in a small high speed water tunnel.

6. PRESENT STATUS OF THE TRANSITION PREDICTION METHOD.

All stability data obtained from [7,8,11] and the inviscid stability calculations mentioned in the preceding section, have been reduced to a table containing about 300 numbers.

Using this table, the amplification rate T can easily be obtained for any velocity profile, as soon as the critical Reynolds number is known.

The present author employs a boundary layer calculation method [5] which for attached flow is similar to Thwaites' method. It contains an extra parameter however, which makes the prediction of the separation position as accurate as for Stratford's two-layer method. In separated flows an integral method is used in which the shape of the separation streamline is prescribed. Both for attached and separated flow the primary profile shape parameter is m/m_{sep} . The critical Reynolds number is a function of m/m_{sep} ; this function is assumed to be equal to that obtained for the Falkner-Skan solutions. From calculations with the full method it has been found that the short-cut method, described in the preceding section, gives a very good approximation in separation bubbles. Furthermore it has been found that the values of σ_1 and σ_2 , when transition occurs near separation are much nearer to the flat plate values than for the second version. It can now be expected that σ_1 and σ_2 will be more or less constant for flows with the same initial disturbances. However, σ_1 and σ_2 may have to vary with the level of initial disturbances due to free stream turbulence and noise.

From curve 3 in fig. 1 and table 1 it follows that $\sigma_1 = 8.3$ and $\sigma_2 = 10.4$ if Schubauer and Skramstad's transition results for the flat plate are used. From Spangler and Wells' experiment on a flat plate in a tunnel with reduced background noise [16,17] and from the authors own experiments somewhat larger values for σ_1 (12) and σ_2 (14.5) would be obtained.

Jaffe, Okamura and Smith [9] applied their solution technique for the Orr-Sommerfeld equation to velocity profiles that had been obtained numerically for two-dimensional and axi-symmetric flows. They find $\sigma_1=8.3$ for the Schubauer and Skramstad results and $\sigma_1=11.8$ for Well's results; for a large number of flows with pressure gradient σ_1 values ranging from 6.8 to 12.1 were obtained. A good overall correlation of transition position was obtained using $\sigma_1=10$.

7. RELATION BETWEEN σ_1 , σ_2 AND FREE STREAM TURBULENCE.

Although it is clear that the initial disturbances cannot be sufficiently characterised by the r.m.s. value of free stream turbulence alone, it will be attempted in the present section to find a relation between σ_1 , σ_2 and the r.m.s. free stream turbulence Tu (in %).

In many different papers relations between Tu , R_{θ} or R_x at transition have been given for the flat plate. The measured transition positions may be converted to σ -values using curve 3 from fig. 1b. Then σ will decrease when Tu increases; fig. 10 shows a collection of these data; for $Tu > 0.1\%$ the relation used by Mack in fig. 3 of [18] can be approximated by:

$$\sigma_1 = 2.13 - 6.18 \log_{10} Tu \quad (7)$$

while for σ_2 a reasonable approximation is:

$$\sigma_2 = 5 - 6.18 \log_{10} Tu \quad (8)$$

For values of $Tu < 0.1\%$ there is much more scatter because in this region sound disturbances may become the factor controlling transition rather than turbulence. We may also use the relations (7) and (8) for $Tu < 0.1\%$; but then we should define an "effective" value for Tu . Of course this does not solve the problem because we can only define an "effective Tu " for a wind tunnel after transition experiments have been made in that same tunnel.

At the time of writing this paper some additional measurements in the low speed low turbulence wind tunnel of the Department of Aerospace Engineering were being performed.

The results of these further investigations are included in the appendix.

For the time being it is suggested to use (7) and (8), assuming an effective Tu equal to 0.1% for modern wind tunnels, resulting in $\sigma_1 = 8.3$ and $\sigma = 11.2$.

8. REFERENCES.

1. Ingen, J.L. van: A suggested semi-empirical method for the calculation of the boundary layer transition region. Report VTH-74, Dept. of Aeron. Eng., University of Technology Delft, 1956.
2. Ingen, J.L. van: Theoretical and experimental investigations of incompressible laminar boundary layers with and without suction. Report VTH-124, Dept. of Aeron. Eng., University of Technology Delft, 1965.
3. Smith, A.M.O. and Gamberoni, N.: Transition, pressure gradient and stability theory. Report ES 26388, Douglas Aircraft Co., 1956.
4. Dobbinga, E., Ingen, J.L. van, Kooi, J.W.: Some research on two-dimensional laminar separation bubbles, AGARD CP-102, paper nr. 2, Lisbon 1972.
5. Ingen, J.L. van: On the calculation of laminar separation bubbles in two-dimensional incompressible flow. In AGARD CP-168: "Flow Separation", Göttingen, 1975.
6. Pretsch, J.: Die Stabilität einer ebenen Laminarströmung bei Druckgefälle und Druckanstieg. Jahrbuch 1941 der deutschen Luftfahrtforschung, I 58.
7. Wazzan, A.R., Okamura, T.T. and Smith, A.M.O.: Spatial and temporal stability charts for the Falkner-Skan boundary layer profiles. DAC 67086, sept. 1968, McDonnell Douglas Corp.
8. Kümmerer, H.: Numerische Untersuchungen zur Stabilität ebener laminarer Grenzschichtströmungen. Dissertation Technische Hochschule, Stuttgart, 1973.
9. Jaffe, N.A., Okamura, T.T. and Smith, A.M.O.: Determination of spatial amplification factors and their application to predicting transition. AIAA Journal, Vol 8, no 2, February 1970, p 301-308.
10. Stratford, B.S.: Flow in the laminar boundary layer near separation. R and M 3002, 1957.
11. Taghavi, H. and Wazzan, A.R.: Spatial stability of some Falkner-Skan profiles with reversed flow. Physics of Fluids, Vol 17, no 12, Dec. 1974, p 2181-2183.
12. Schubauer, G.B. and Skramstad, H.K.: Laminar boundary layer oscillations and transition on a flat plate. NACA Rept 909, 1948.
13. Ingen, J.L. van: Advanced computer technology in aerodynamics; a program for airfoil section design utilizing computer graphics. VKI Lecture series 16 on High Reynolds number subsonic aerodynamics, April 21-25, 1969.
14. Boermans, L.M.M. and Blom, J.J.H.: Low-speed aerodynamic characteristics of an 18-percent-thick airfoil section designed for the all-flying tailplane of the M300 sailplane. Report LR-226, Department of Aerospace Eng., Delft University of Technology, 1976.
15. Van der Meulen, J.H.J.: A holographic study of cavitation on axi-symmetric bodies and the influence of polymer additives. Doctoral Thesis, University of Technology Twente, 1976.
16. Wells, C.S.: Effects of free stream turbulence on boundary layer transition. AIAA Journal, Vol. 5, No 1, January 1967, p 172-174.
17. Spangler, J.G. and Wells, C.S.: Effects of free stream disturbances on boundary-layer transition. AIAA Journal, Vol 6, No 3, March 1968, p 543-545.
18. Mack, L.M.: A numerical method for the prediction of high-speed boundary-layer transition using linear theory. Paper nr. 4 in Aerodynamic analysis requiring advanced computers; NASA SP-347, 1975.
19. Hall, D.J. and Gibbings, J.C.: Influence of stream turbulence and pressure gradient upon boundary layer transition. Journal Mechanical Engineering Science, Vol 14, no 2, 1972, p 134-146.

9. ACKNOWLEDGEMENT.

The author is indebted to professor A.R. Wazzan for making available some tabular material concerning the stability of reversed flows. Ir. J.J.H. Blom should be thanked for his active participation in the preparation of this paper.

Table 1: Critical values for σ at beginning (σ_1) and end of the transition region (σ_2) on a flat plate according to different stability calculations. Transition Reynolds numbers 2.8 and 3.9×10^6 according to [12].

curve no in fig. 1b	σ_1	σ_2	stability diagram used
1	7.6	9.7	Pretsch, flat plate ($\beta=0$); version 1.
2	9.2	11.2	Pretsch, stability diagram for $10 \log\left(\frac{U_0}{v}\right)_{crit} = 2.345$ which according to Lin's formula would apply to the flat plate velocity profile in version 2.
3	8.3	10.4	from [7] and [8]

Table 2: z and I as a function of the Hartree shape parameter β for reversed flows.

β	$z = z_{sep}$	I
-.198838	0	127
-.198	.042	145
-.197	.061	154
-.195	.088	167
-.190	.134	190
-.180	.199	225
-.160	.307	285
-.150	.360	315
-.140	.420	348
-.120	.556	422
-.100	.682	483
-.075	1.107	659
-.050	1.864	883
-.025	4.249	1331

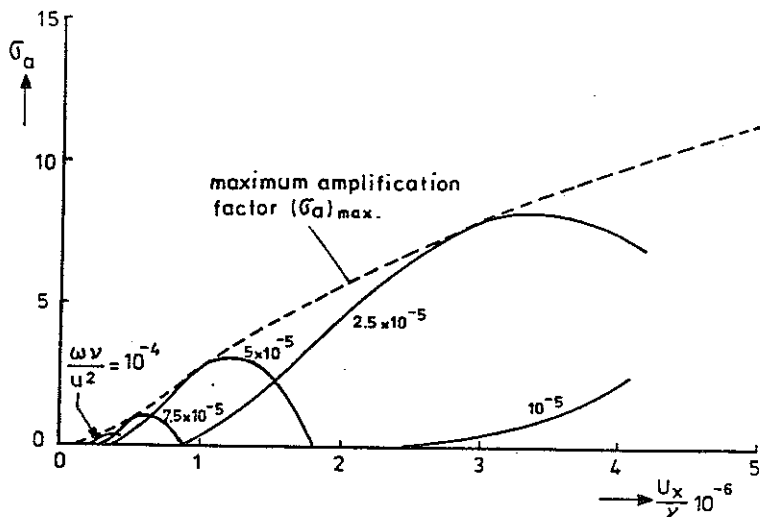


Fig. 1a.
Amplification factor for the flat plate according to Pretsch [6].

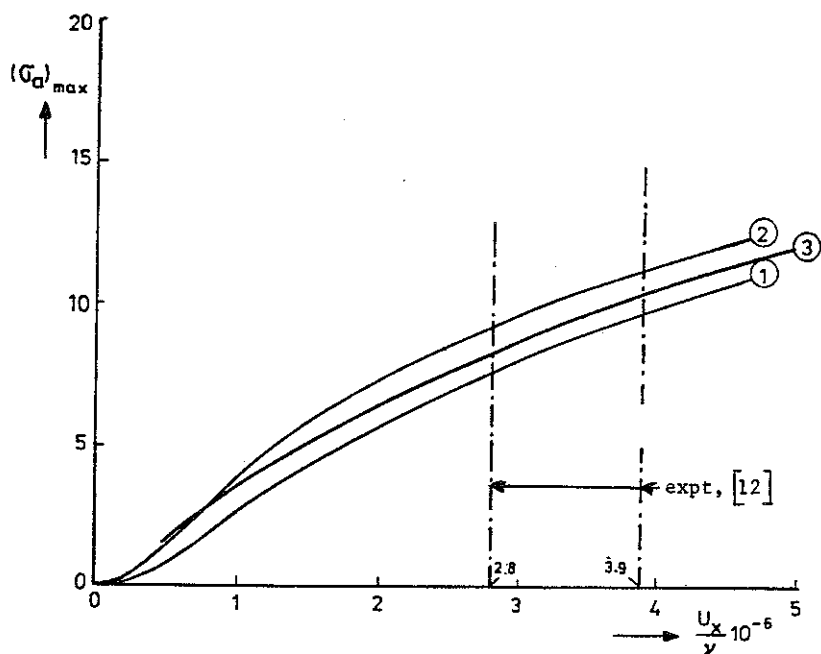


Fig. 1b.
Maximum amplification factor for the flat plate according to different stability calculations (see also table 1).

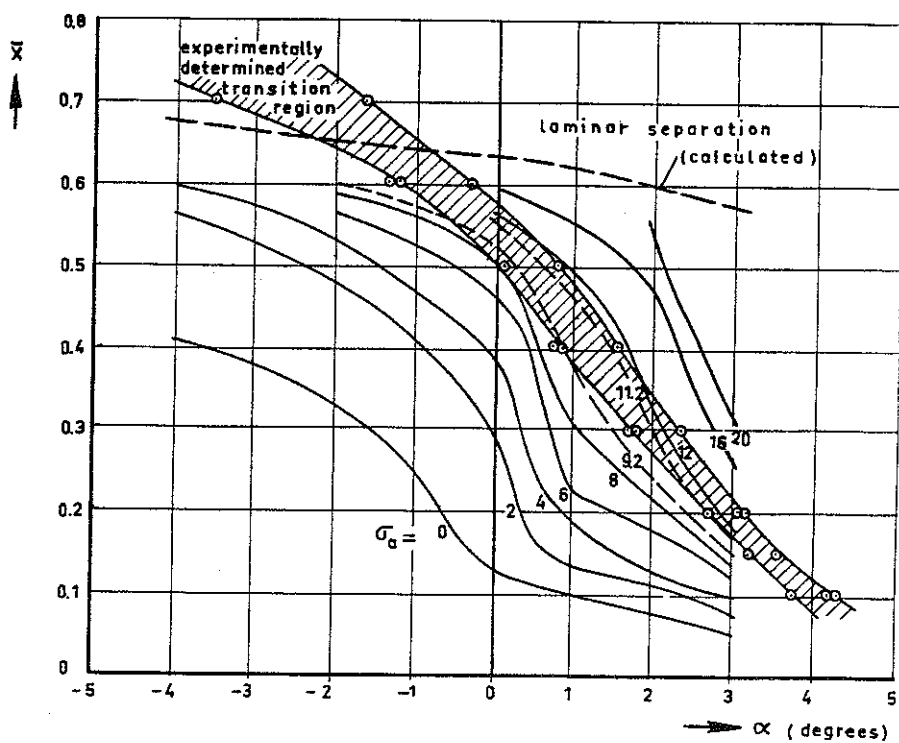


Fig. 2.
Calculated amplification factor and measured transition region for the EC 1440 airfoil section.

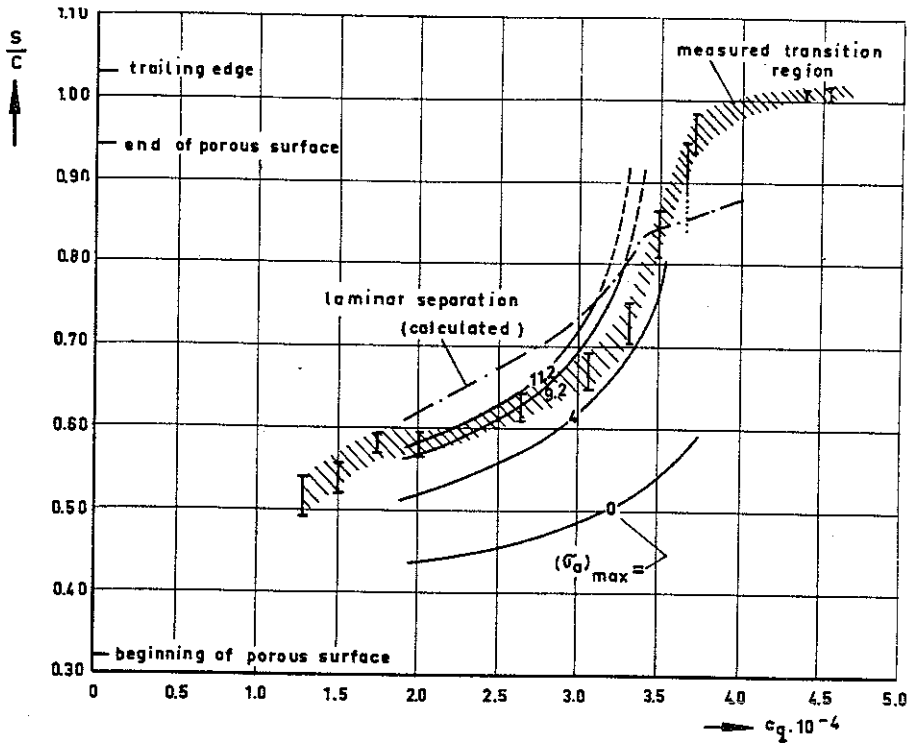


Fig. 3. Measured transition and calculated amplification factor for the upper surface of the suction model, $\alpha=0^\circ$, $R_c=3.37 \times 10^6$ (c_{qu} is the suction flow coefficient for the upper surface; $c_q = \frac{Q}{U_\infty c}$; Q is volume flow of sucked air per unit span).

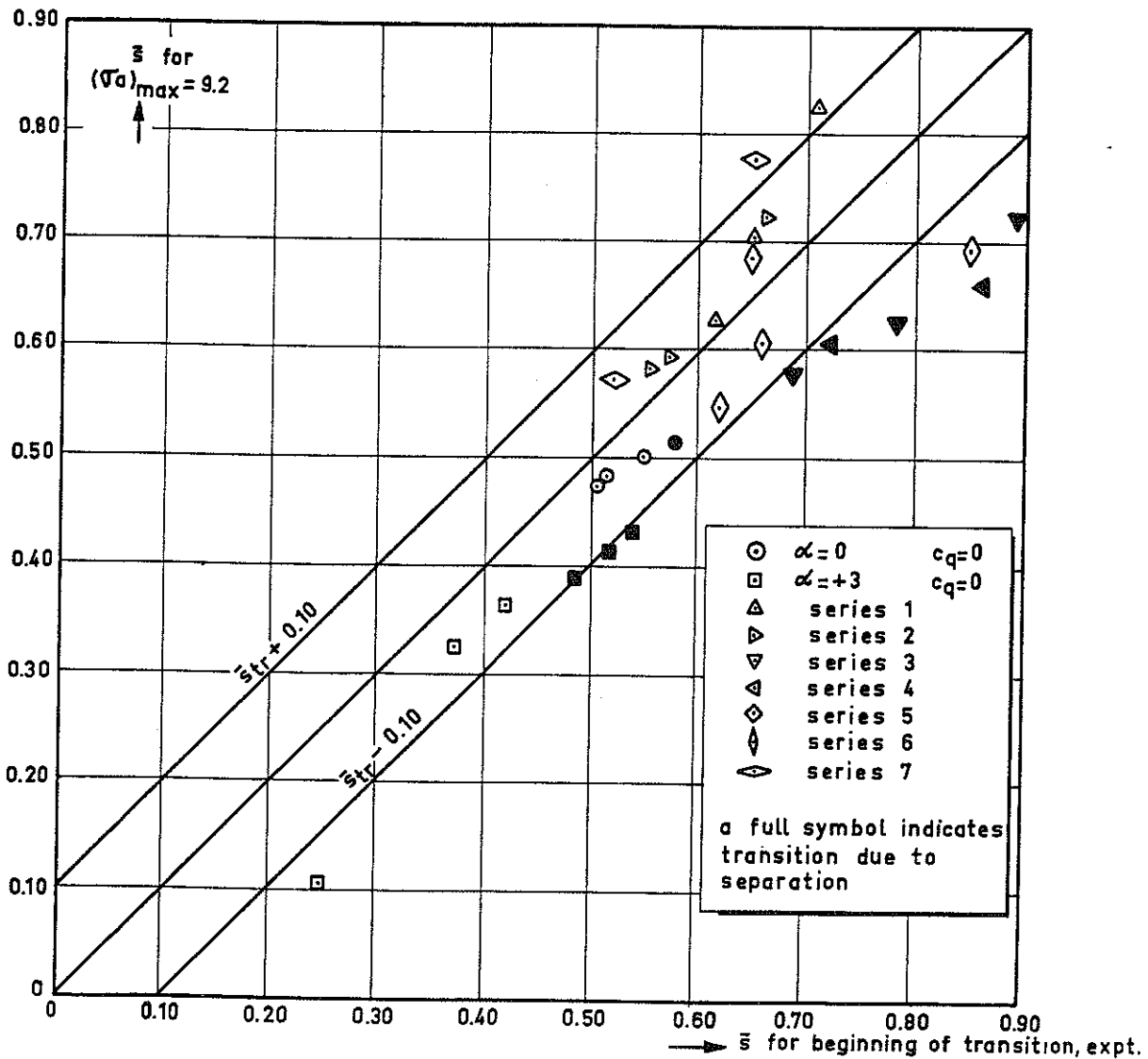


Fig. 4: Summary of measured and calculated positions of the beginning of transition for the airfoil with suction [2].

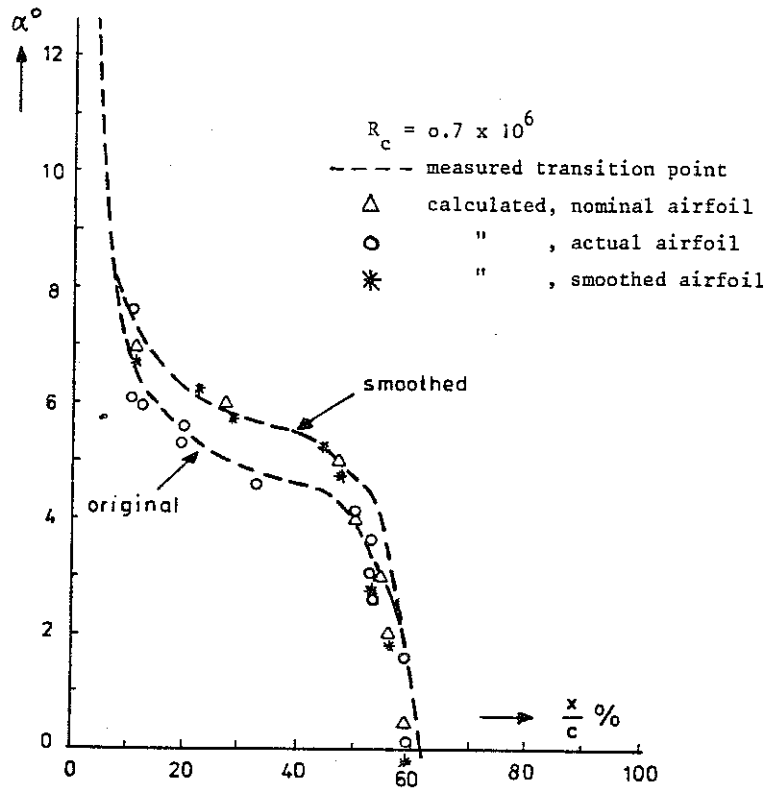


Fig. 5: Comparison between theory and experiment for the upper surface of the M-300 airfoil [14].

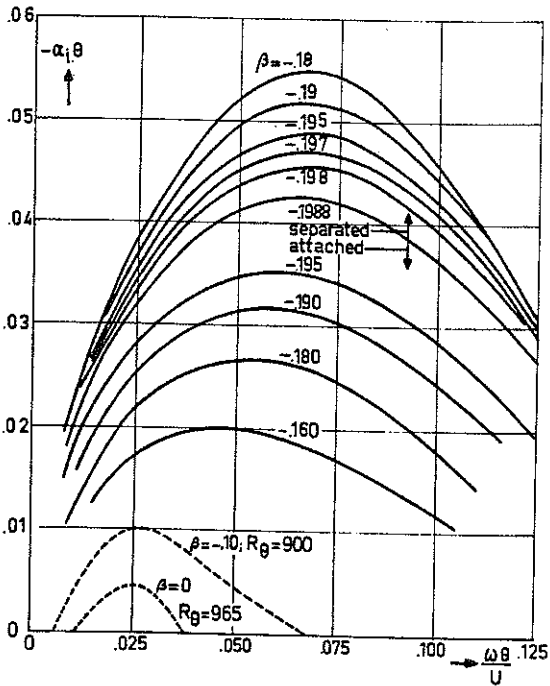


Fig. 6: Attached and separated flow.

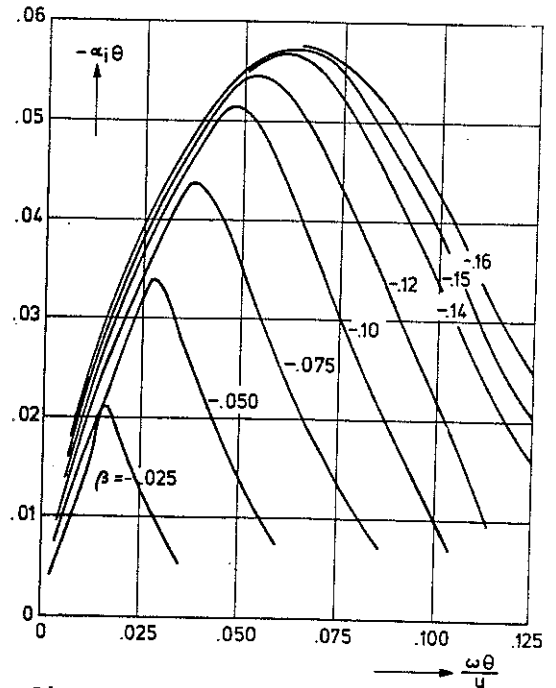


Fig. 7: Separated flow.

Figs 6 and 7: Inviscid instability for Hartree's and Stewartson's velocity profiles. For attached flow $-\alpha_i \theta \rightarrow 0$ for $\beta \rightarrow 0$, for comparison the viscid instability is shown for $\beta = 0$ and -10 when R_θ is about 1000.

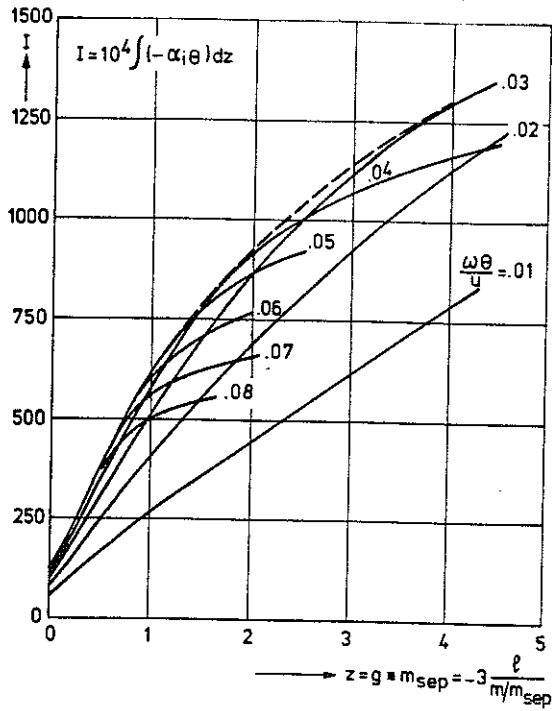


Fig. 8: Amplification integral I

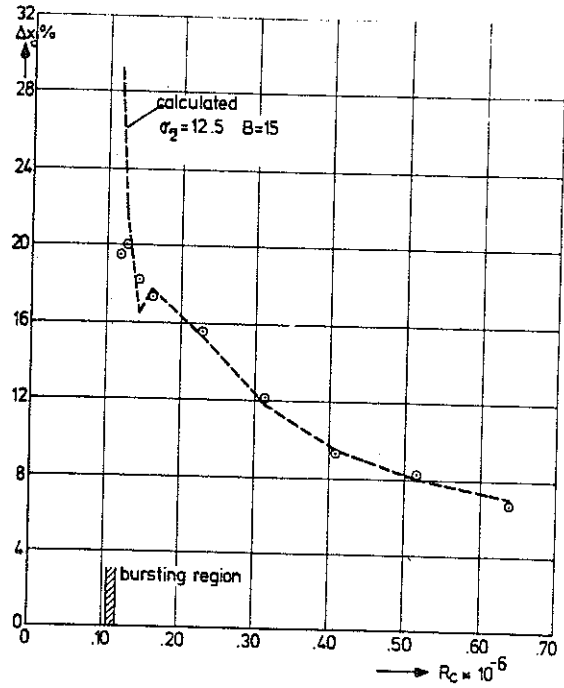


Fig. 9: Distance between separation and transition on a Wortmann airfoil in a small "noisy" wind tunnel.

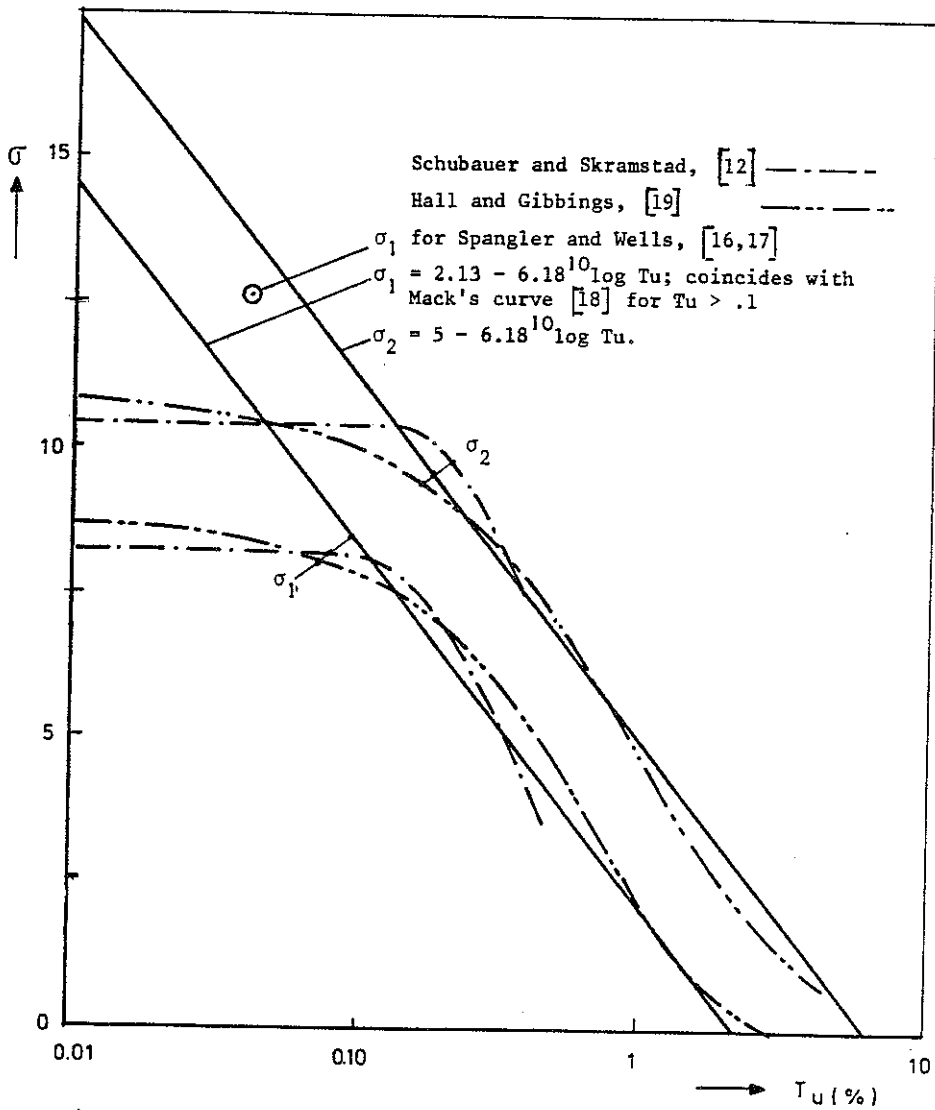


Fig. 10: Relation between σ_1 , σ_2 and T_u for the flat plate.

APPENDIX: SOME FURTHER RESULTS.

Between the time of writing the main text of the present paper and the actual presentation a further analysis has been performed. Some of its results are given in this appendix.

In fig. 11 some results are given for the length of the laminar part of the bubble Δx , non-dimensionalised with θ_{sep} as function of $R_{\theta_{sep}}$.

The measurements refer to:

- series 1: ● , Wortmann airfoil FX 66-S-196 V1, $\alpha=1^\circ$ in a small noisy tunnel,
- series 2: ○ , Wortmann airfoil FX 66-S-196 V1, $\alpha=1^\circ$ in a large low turbulence tunnel,
- series 3: □ , circular cylinder with tail (configuration c from [4]) in a large low turbulence tunnel,
- series 4: △ , same as series 3 but noise from the small tunnel recorded on a tape recorder and reproduced in the test section of the large low turbulence tunnel.

The grids superimposed on fig. 11 and subsequent figs. will be discussed later. It is clear from fig. 11 that no single curve can be drawn through the experimental points. Hence there must be additional parameters, besides $R_{\theta_{sep}}$, which govern $\Delta x/\theta_{sep}$. Certainly free stream turbulence and noise must be important. We will try to correlate these results by using the "effective turbulence level". Tu , as introduced in section 7, as an additional parameter. In fact this parameter will act as a "figure of merit" for the facility in which the measurements have been performed. Through equation (8) the values of Tu and σ_2 can be related. It should be stressed that the "effective" Tu is not necessarily equal to the free stream turbulence level according to the conventional definition. Noise should be added while parts of the turbulence spectrum which are not dangerous in the sense of Tollmien-Schlichting instability should be subtracted. In other words; the "effective Tu " can only be determined from experiments in each facility.

The way in which results have been plotted in fig. 11 suffers from a large amount of scatter. This is shown in fig. 12, where the effect of errors in Δx of $\pm 0.5\%$ chord are indicated for series 2. Plotting the results as in fig. 13 gives a much more constant width of the scatter band. A more fundamental reason to use $\xi = \frac{\Delta x}{\theta_{sep} R_{\theta_{sep}}}$ as a new independent variable is that using ξ and $\bar{y} = y/\theta_{sep}$ (and similar scaling for u and v) makes the boundary layer equations independent of Reynoldsnumber.

Assuming:

- a. that amplification of unstable disturbances only occurs within the bubble and a short distance upstream of separation (this is the case for a relatively strong favourable pressure gradient followed by separation due to a sudden adverse pressure gradient),
- b. that the pressure distribution within the laminar part of the bubble and a short distance upstream of separation, plotted as U/U_{sep} vs. ξ is universal (our own unpublished measurements - although there is a large amount of scatter - encourage us to make this assumption),
- c. that the velocity profile at separation is universal when using y/θ_{sep} as coordinate normal to the wall,

it is easy to show that the amplification factor σ can be written as:

$$\sigma = R_{\theta_{sep}} F(\xi) \quad (9)$$

where $F(\xi)$ is a universal function of ξ .

We may also write eq. (9) as:

$$\frac{10^4}{R_{\theta_{sep}}} = \frac{10^4 F(\xi)}{\sigma} \quad (10)$$

Hence when σ would be known at transition in the bubble, $F(\xi)$ might be determined from our measurements. Assuming only that σ is a constant at transition induces us to plot $10^4/R_{\theta_{sep}}$ as a function of ξ . This in fact has been done in fig. 13.

When further

- d. the short cut method (section 5 of main paper) with $B=17.5$ and $m_{sep} = 0.10$ is used, we can calculate $F(\xi)$.

The result is shown in fig. 14. Because the parallel flow assumption has been made in the stability calculations which have been used and moreover the accuracy of the short-cut method is not known for large values of ξ , the shape of $F(\xi)$ for large values of ξ is uncertain. Therefore we are emboldened to replace $F(\xi)$ by the linear approximation (see fig. 14):

$$10^4 F(\xi) = 70 + 530\xi \quad (11)$$

Hence (9) and (11) lead to:

$$\sigma = R_{\theta \text{ sep}} 10^{-4} (70 + 530\xi) \quad (12)$$

or:

$$\frac{10^4}{R_{\theta \text{ sep}}} = \frac{70 + 530\xi}{\sigma} \quad (13)$$

It follows that for constant σ at transition the linear relation between ξ at transition and $10^4/R_{\theta \text{ sep}}$, as shown in fig. 13, is reproduced by eq. (13).

The results of fig. 11 have been replotted in fig. 15, the superimposed grid in fig. 15 and in earlier figures is based on eq. (13). The values of the "effective Tu", mentioned in these figures have been calculated from eq. (8).

It follows that σ and hence Tu are reasonably constant for each series of measurements. Between the different series differences in effective Tu occur.

Using the relation (8) between Tu and σ_2 and relation (12) between σ_2 and ξ we can predict the position of transition in a bubble which is formed due to a sudden adverse pressure gradient following a rather strong favourable pressure gradient. For cases where an appreciable amount of amplification occurs upstream of separation, the full version of the amplification calculation method (section 6) should be used.

Combining this transition method with a method to predict whether reattachment will occur (proposed in section 7 of [5]; the method uses Stratford's limiting pressure distribution as a discriminator) we are now able to predict bursting of the bubble. This method appears to work quite well for bubbles occurring near midchord on airfoils at low angles of attack.

However, when trying to predict bursting for the NACA 63-009 airfoil (see Gault, NACA TN-2502) the method failed. It is possible that curvature effects on the transition and reattachment processes are important. Moreover, Mach number effects may be important for cases where very high suction peaks occur. It should also be observed that the "effective" Tu may be very low for these cases because the turbulence at the edge of the boundary layer may be damped due to the very strong flow acceleration towards the suction peak. Also the dangerous Tollmien-Schlichting frequencies are very high for these cases and possibly higher than those occurring with sufficient energy in the free stream turbulence spectrum.

It should be stressed again that the "effective" Tu cannot be taken equal to the free stream turbulence level as conventionally defined. A striking illustration of this remark is provided by the results of some additional measurements^{x)} for series 1. The free stream turbulence level was increased to values between 0.5% and 1% by means of screens. No appreciable reduction of the laminar part of the bubble was observed. This can only be explained by the mismatching of the added turbulence with the most amplified Tollmien-Schlichting waves. In other words increasing Tu does not always mean increasing the "effective Tu". This leaves us with the problem that the effective Tu can only be obtained from experiments in each wind tunnel for a number of representative cases.

When results of such measurements are not available the suggestion at the end of the main text of the paper might be followed.

^{x)} These measurements have been performed by mr. J.C.M. Hazebroek, student in the Department of Aerospace Eng.

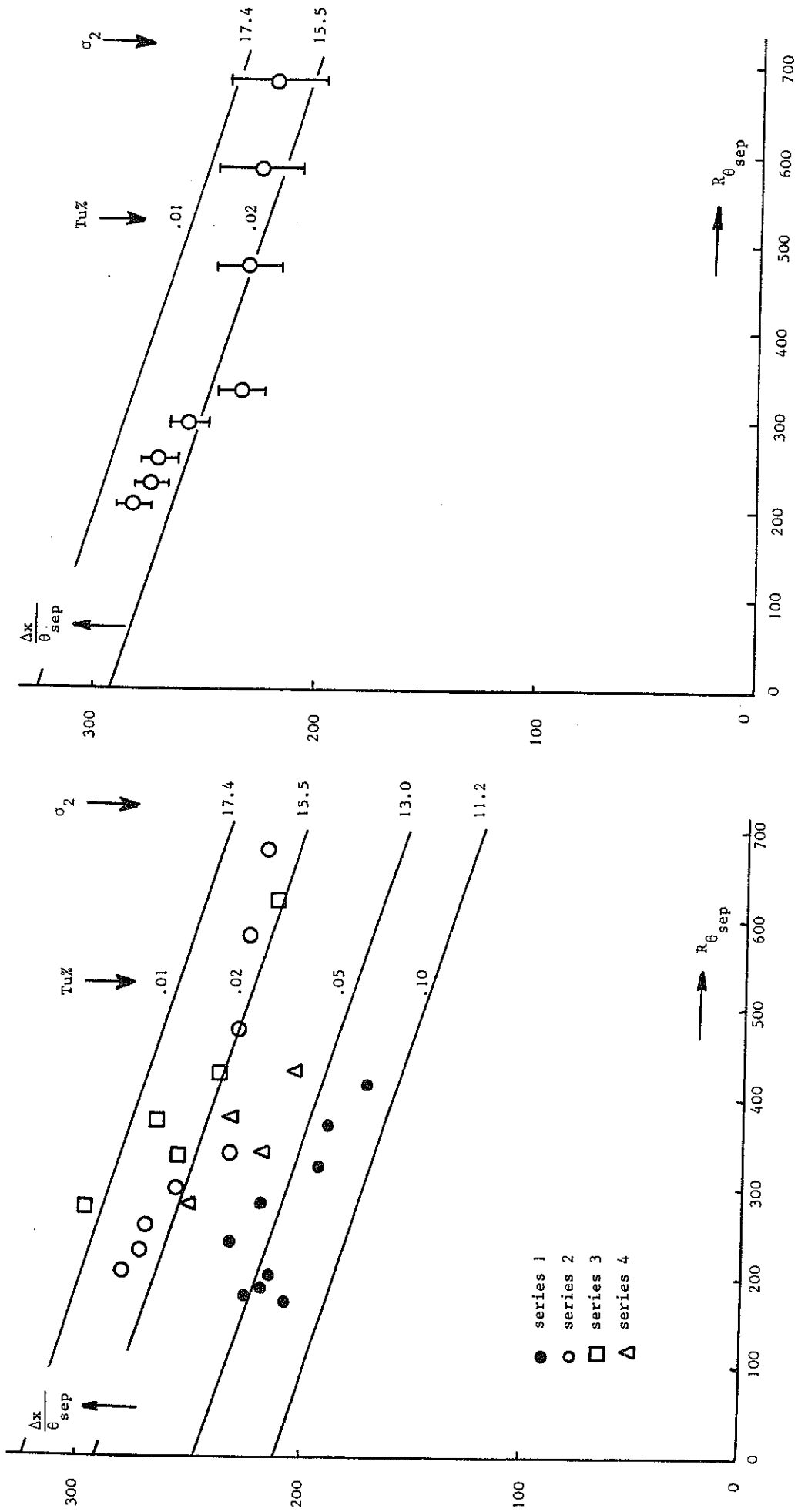


Fig. 11: Length of the laminar part of the bubble.

Fig. 12: Length of the laminar part of the bubble for series 2; bars indicate errors in Δx of + or - 0.5% chord.

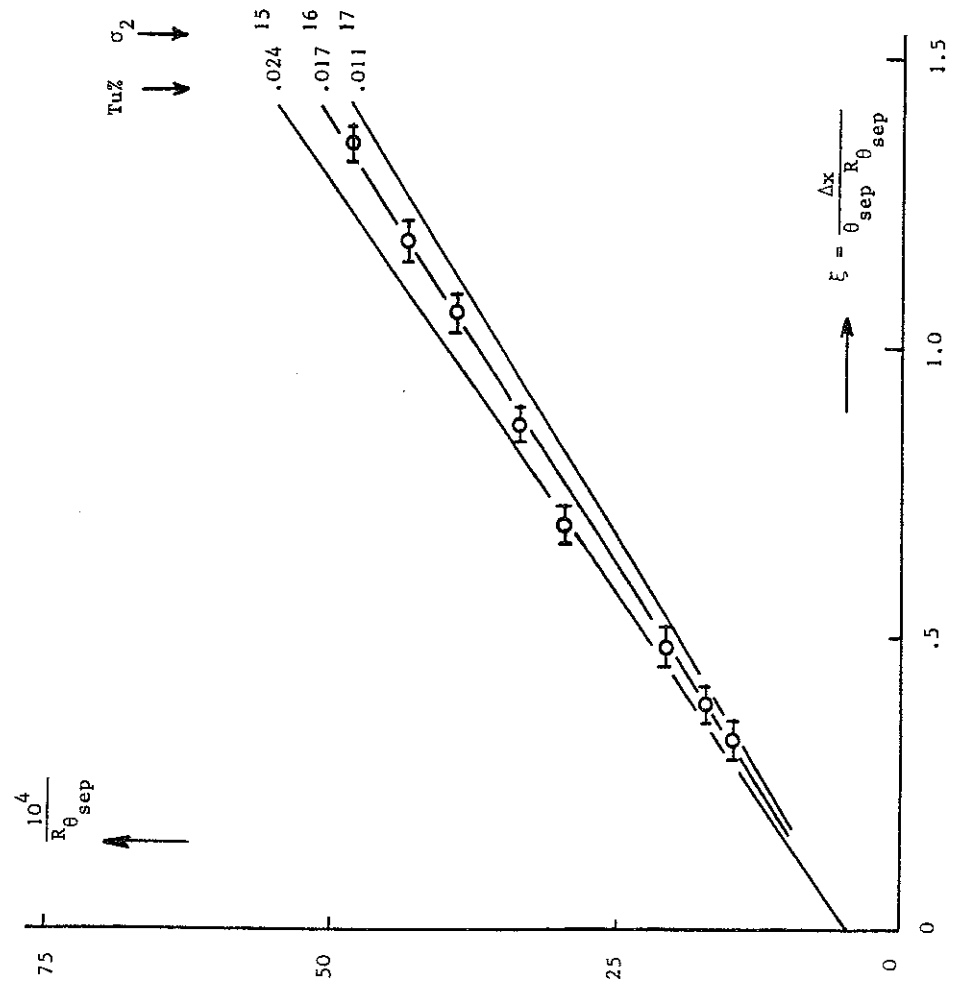


Fig. 13: Results for series 2; bars indicate errors in Δx of $\pm 0.5\%$ chord.

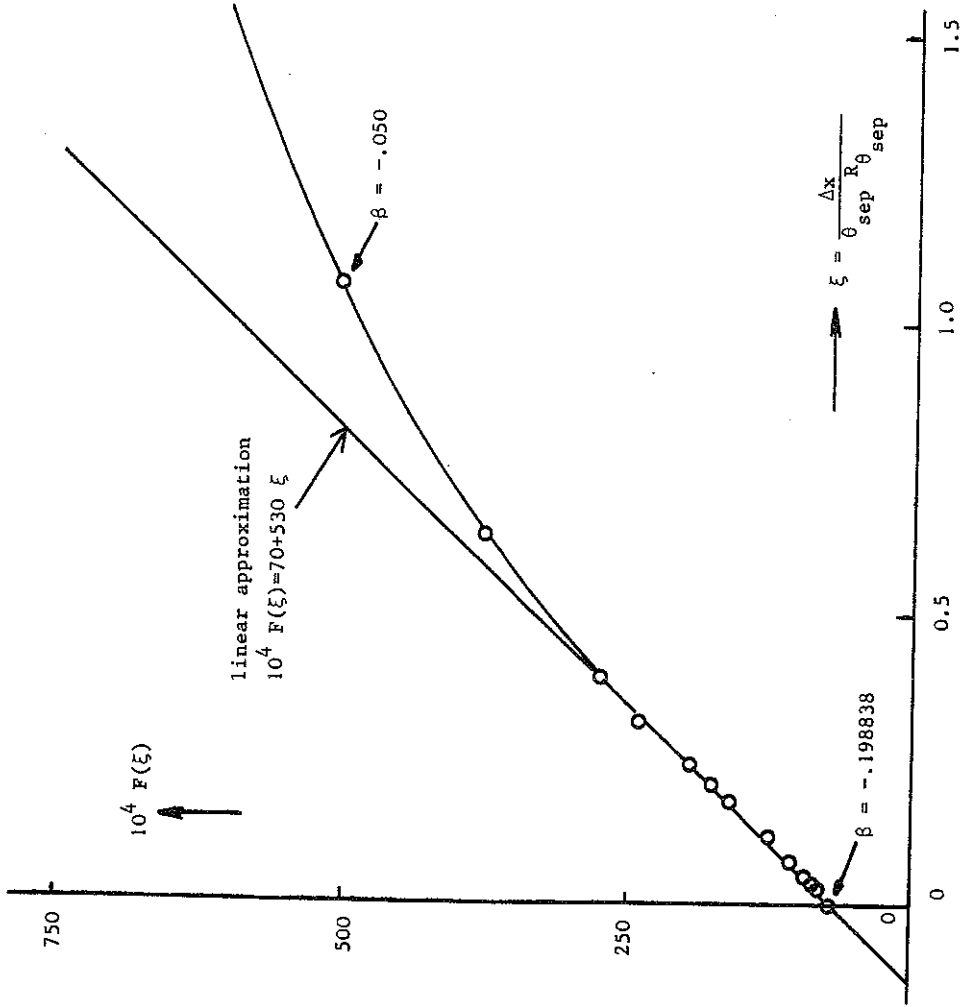


Fig. 14: $F(\xi)$ according to the short cut method; symbols - 0 - correspond to the values of I taken from table 2 for $\beta = -.198838$ through $-.050$; $B = 17.5$; $m_{\text{sep}} = 0.10$.

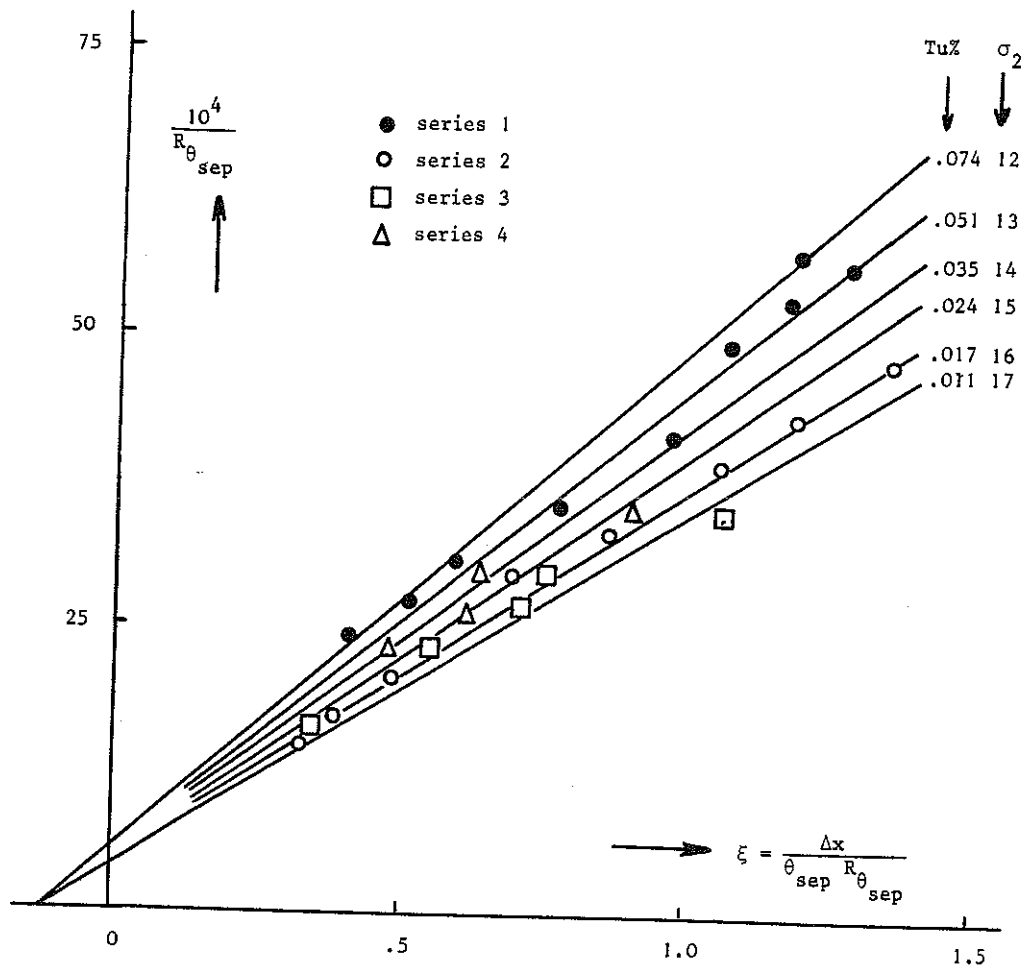


Fig. 15: Length of the laminar part of the bubble correlated with "effective Tu" and σ_2 .